

# Impact of warming and deoxygenation on the habitat distribution of Pacific halibut in the Northeast Pacific

Ana C. Franco<sup>1</sup> | Hongsik Kim<sup>2</sup> | Hartmut Frenzel<sup>3\*†</sup> |  
Curtis Deutsch<sup>3‡</sup> | Debby Ianson<sup>4</sup> | U. Rashid Sumaila<sup>2</sup>  
| Philippe D. Tortell<sup>1,5</sup>

<sup>1</sup>Department of Earth, Ocean and Atmospheric Sciences, University of British Columbia, Vancouver, British Columbia, Canada

<sup>2</sup>Fisheries Economics Research Unit, University of British Columbia, Vancouver, British Columbia, Canada

<sup>3</sup>School of Oceanography, University of Washington, Seattle, Washington, USA

<sup>4</sup>Institute of Ocean Sciences, Fisheries and Oceans Canada (DFO), Sidney, British Columbia, Canada

<sup>5</sup>Department of Botany, University of British Columbia, Vancouver, BC, Canada

**Correspondence**

Email: afranco@eoas.ubc.ca

**Present address**

\*Cooperative Institute for Climate, Ocean and Ecosystem Studies, University of Washington, Seattle, Washington, USA

†Pacific Marine Environmental Laboratory, National Oceanic and Atmospheric Administration, Seattle, Washington, USA

‡Department of Geosciences, Princeton University, Princeton, New Jersey, USA

**Funding information**

Ocean warming and deoxygenation are already modifying the habitats of many aerobic organisms. Benthic habitat in the Northeast Pacific is sensitive to deoxygenation, as low oxygen concentrations occur naturally in continental shelf bottom waters. Here we examine the potential impacts of deoxygenation and ocean warming on the habitat distribution of Pacific halibut (*Hippoglossus stenolepis*), one of the most commercially-important groundfish in North America. We combine fisheries-independent Pacific halibut survey data (1998 – 2020) with oceanographic measurements and a regional ocean circulation model to investigate current and future (end of 21<sup>st</sup> century) influences of deoxygenation and warming on optimal Pacific halibut habitat. We use the observations and model output to derive a metabolic index of Pacific halibut-specific suitable habitat. Our results show high Pacific halibut counts in regions where the metabolic index is greatest, and demonstrate that interannual variability in Pacific halibut abundance is coherent with the Pacific Decadal Oscillation. Working with model projections, we examine potential future changes in suitable Pacific halibut habitat by the end of the century under a

This is the author manuscript accepted for publication and has undergone full peer review but has not been through the copyediting, typesetting, pagination and proofreading process. This may lead to differences between this version and the Version of Record. Please cite this article as doi: [10.1111/fog.12610](https://doi.org/10.1111/fog.12610)

high carbon dioxide emissions scenario. These projections indicate that suitable Pacific halibut habitat may largely disappear off the coast of Washington state, retreating approximately five degrees latitude northward. In bottom waters along coastal British Columbia and Alaska continental shelf, Pacific halibut habitat is projected to decrease by about 50%. Such habitat changes may potentially drive a northward shift in Pacific halibut, with significant implications for commercial fisheries.

#### KEYWORDS

Pacific halibut, Metabolic index, oxygen demand, ocean warming, ROMS, Subarctic Pacific

## 1 | INTRODUCTION

Ocean warming and deoxygenation are already modifying habitat availability for many aerobic organisms, with significant impacts on their distribution over space and time (Cheung et al., 2009; Keeling et al., 2010; Seibel, 2011). A number of studies have analyzed the response of marine species distributions and ecosystem structure to increasing temperature (Campana et al., 2020; Christian and Holmes, 2016; McLean et al., 2018; Perry et al., 2005; Sunday et al., 2015), but less work has considered the impact of concurrent warming and deoxygenation in driving habitat reduction (Bianucci et al., 2015; Deutsch et al., 2015, 2020; Howard et al., 2020b; Thompson et al., 2022).

From both a physiological and oceanographic perspective, oxygen availability and temperature are closely linked. Physiologically, the metabolic oxygen demand of aerobic organisms rises with increasing temperature (Pörtner and Knust, 2007), such that deoxygenation has greater impacts on organismal growth and survival under high temperature conditions (Deutsch et al., 2015, 2020). At the same time, higher temperature favors oxygen loss by decreasing seawater oxygen solubility and increasing stratification, which limits the ventilation rate of thermocline water masses (Franco et al., 2021; Kwon et al., 2016; Ono et al., 2001; Sasano et al., 2018). Among all oceanic regions, the Northeast Pacific exhibits one of the most rapid apparent rates of deoxygenation (Keeling et al., 2010; Schmidtke et al., 2017), with large oxygen decreases projected for intermediate depths over the coming decades (Long et al., 2016). This ocean region has already lost approximately 15% of its oxygen inventory over the past 60 years (Ross et al., 2020), but it is presently unclear how ecosystem structure and species distributions have been impacted.

The habitat of benthic organisms is particularly sensitive to deoxygenation (Levin et al., 2009; Ross et al., 2020; Yati et al., 2020) since low oxygen concentrations occur naturally in the subsurface waters due to respiration of organic matter. Near the coast, increased nutrient input and subsequent eutrophication, exacerbate coastal deoxygenation and modify nutrient and microbial cycles (Breitburg et al., 2018; Gilly et al., 2013; Howarth et al., 2011). Among fish species, groundfish, which spend the majority of their adult life near the ocean floor, are thus most susceptible to oxygen depletion. For example, a recent study using numerical biogeochemical ocean models and fisheries observations showed that future anthropogenic deoxygenation and warming may drive biodiversity changes on groundfish species in the North Pacific (Thompson et al., 2022). Similarly, Bianucci et al. (2015) demonstrated that decreasing oxygen concentration in the Gulf of St. Lawrence led to a reduction in the optimal habitat of the groundfish Atlantic wolffish

60 and associated changes in its distribution. Using similar numerical and observational tools and accounting for future  
61 projected changes in temperature and oxygen, Clarke et al. (2021) showed that commercially-important fisheries in  
62 the Eastern tropical Pacific will also be affected by habitat contraction. Howard et al. (2020b) estimated that ocean  
63 warming and deoxygenation can potentially drive widespread extirpation of northern anchovy, a key forage species  
64 in the California Current System.

65 Commercial groundfish fisheries account for approximately 50% of the total fish landings in the US (Lehodey  
66 et al., 2006). The Pacific halibut (*Hippoglossus stenolepis*) fishery is one of the most important commercial groundfish  
67 fisheries along the Northwest coast of the United States and Canada (Haigh et al. (2015), their Figure 4). This species  
68 is distributed over the majority of the North American Pacific coast, from central California to the Bering Sea (Sadorus  
69 et al., 2021), and is regulated and surveyed by the International Pacific Halibut Commission (IPHC). Since 1997, the  
70 number of Pacific halibut counted in fisheries-independent surveys has declined persistently along the entire IPHC  
71 regulatory areas, from Alaska to California (Stewart and Wilson, 2020). Regionally, however, Pacific halibut catch per  
72 unit effort (CPUE) in the coastal waters of California, British Columbia, and Southeast Alaska, has varied significantly  
73 across years, with no apparent trend between 1992 to 2019 (Stewart and Wilson, 2020).

74 A number of oceanographic variables, including bottom depth, temperature and dissolved oxygen are all likely im-  
75 portant factors influencing Pacific halibut distribution and abundance (Sadorus et al., 2014). To date, however, there  
76 have been few studies explicitly examining regional-scale links between oceanographic conditions and Pacific halibut  
77 abundance. Earlier work demonstrated that interannual variability in Pacific halibut recruitment, growth and distribu-  
78 tion may be linked to the Pacific Decadal Oscillation (PDO) (Mantua et al., 1997; Francis and Hare, 1994), an index  
79 describing a pattern of ocean-atmosphere variability. In the Northeast Pacific, a positive PDO phase translates into  
80 warmer surface temperatures and higher stratification, while the opposite occurs during a negative (i.e., cold) phase  
81 (Chhak and Di Lorenzo, 2007). Using one of the longest Pacific halibut time series available (1935 to 1994), Clark  
82 and Hare (2002) showed that the abundance of the six-year age class Pacific halibut increased when the fish were  
83 spawned during positive regimes of the PDO, while the opposite occurred during negative phases of the PDO. This  
84 result suggests that processes driven by the PDO may influence the synchrony between groundfish spawning, recruit-  
85 ment and climatic indices (Lehodey et al., 2006). However, the underlying factors driving this empirical relationship  
86 remain unknown.

87 Here we build on previous work, combining fisheries-independent survey data with oceanographic observations  
88 and a regional ocean model to examine the relationship between environmental factors and Pacific halibut CPUE. We  
89 focus particular attention on the relationship between Pacific halibut distribution and the oxygen and temperature  
90 properties in coastal ocean bottom waters off California to Southeast Alaska. By examining the historical trends,  
91 present-day spatial distributions, and potential future trajectories, our goal is to explore potential climate change  
92 impacts on the future distribution of Pacific halibut habitat and habitat suitability in an ecological and economically  
93 important ocean region.

## 94 2 | DATA AND METHODS

### 95 2.1 | Pacific halibut data

96 Observations of Pacific halibut CPUE were obtained from the IPHC Fishery-Independent Setline Surveys (FISS)  
97 (<https://www.iphc.int/data/fiss-data-query>), for the subareas 2A (off California, Oregon and Washington, USA), 2B  
98 (off British Columbia, Canada) and 2C (off Prince of Wales Island, Alaska, USA). These subareas (shown in Figure 1)  
99 were operationally established by the IPHC in 1990 for the management of the fishery. Each subarea extends 200

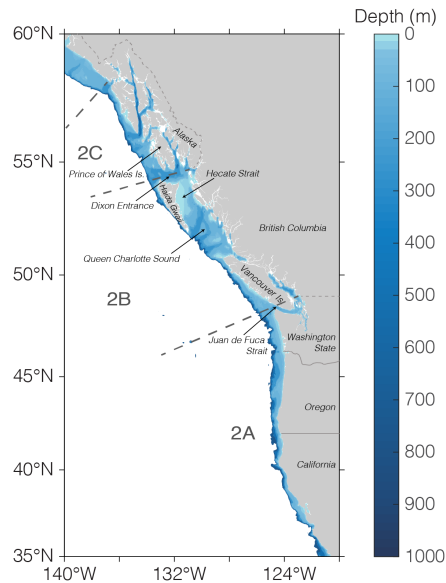


**FIGURE 1** Reference map showing the IPHC Regulatory subareas 2A, 2B, and 2C and other relevant geographical features. The color scale represents the ocean bathymetry in the Pacific halibut sampling region up to 1000 m depth. Dashed lines on land indicate the Canada - USA borders, while dashed lines in the ocean indicate IPHC subarea boundaries. The southern boundary of subarea 2A extends to the international border between US and Mexico, however, the FISS stations are limited to north of 37°N.

100 nautical miles offshore, but the majority of the sampling stations are located over the continental slope within 150 km  
 101 (approximately 80 nautical miles) from the coast.

102 Most sampling stations were visited each summer (June - August), when Pacific halibut approach the coast to  
 103 feed (Skud, 1977). The majority of the stations were sampled at least 20 times over the 23-year period of the time  
 104 series, and only stations sampled more than five times over the sampling period (1998-2020) were used to derive  
 105 long-term CPUE summer means. The number of times each station was visited over the sampling period is shown in  
 106 Figure S1. With this criterion, we included 106 stations sampled in subarea 2A, 170 stations in subarea 2B and 123  
 107 stations in subarea 2C. The model grid used to assess the temperature and oxygen characteristics of each region (see  
 108 Section 2.3) does not resolve the inshore waters of the coastal fjords (Figure S2). For this reason, we excluded the  
 109 innermost FISS stations when co-locating fisheries data with model-based environment data (Section 3.1.3). Most of  
 110 these inner stations correspond to stations with the lowest Pacific halibut counts.

111 The Pacific halibut survey data are normalized by the Catch Per Unit Effort (CPUE), which is based on the number  
 112 of effective skates hauled, and where 1 skate is approximately 100 hooks. We report the data as individuals per skate  
 113 (ind./skate), i.e., the CPUE, which may be used as an index of relative abundance, rather than absolute abundance  
 114 (Maunder et al., 2006; Thompson et al., 1998). Sampling details are indicated in the IPHC Fishery-Independent Setline  
 115 Survey Sampling Manual (IPHC, 2021). Pacific halibut CPUE is reported for two size classes; fork lengths greater or less  
 116 than the minimum legal-size limit of 32 inches (81.3 cm). In the following, we consider each size class independently  
 117 and refer to each as over 32 inches (O32) or under 32 inches (U32).

## 118 2.2 | Hydrographic data from IPHC

119 Starting in 2009, hydrographic data (temperature, salinity and dissolved oxygen) have been recorded alongside the  
120 Pacific halibut longline surveys described above. These environmental data were collected at most of the FISS sta-  
121 tions with calibrated SBE19plusV2 water column profilers (Sadorus et al., 2016). We used the deepest readings  
122 from each profile (estimated to be 5-15 m from the sea bottom) as provided from the IPHC data request portal  
123 (<https://www.iphc.int/data/fiss-data-query>). The environmental data reflect the environmental conditions of Pacific  
124 halibut habitat at the time of sampling, and were used to estimate critical statistical parameters describing the suitable  
125 aerobic habitat of Pacific halibut (see Section 2.4).

## 126 2.3 | Model description and simulations

127 To assess the impact of present-day variability and potential future changes in the habitat distribution of Pacific hal-  
128 ibut, we used monthly output from two regional ocean model simulations: 1) a hindcast simulation representing the  
129 period 1994 – 2007, with spatial resolution of 12 km over the whole domain of the IPHC subareas 2A, 2B and 2C; and  
130 2) a 12 km resolution future simulation for the same domain, representing late 21<sup>st</sup> century conditions under the Rep-  
131 resentative Concentration Pathway (RCP) 8.5 (high CO<sub>2</sub> emissions scenario). Currently, the historical total cumulative  
132 CO<sub>2</sub> emissions are consistent with the CO<sub>2</sub> emissions considered in the RCP8.5 (Schwalm et al., 2020). It is expected  
133 that continuing on the RCP8.5 path will lead to a global mean surface air temperature increase of approximately 4°C  
134 (relative to 1986-2005) by the end of the century (Collins et al., 2013), resulting in a large decrease in seawater oxygen  
135 solubility and concentration (Oschlies, 2021). Each Pacific halibut sample was co-located with simulated temperature,  
136 O<sub>2</sub>, and  $\Phi$  in space and time over the period of overlap between the fisheries surveys (1998-2020) and the hindcast  
137 model simulation (1994-2007).

138 The model simulations are based on the Regional Ocean Modeling System (ROMS) (Shchepetkin and McWilliams,  
139 2005), coupled to the Biogeochemical Elemental Cycling (BEC) (Moore et al., 2001, 2004). The model is configured  
140 for the California Current System (CCS), and uses a spherical grid with horizontal resolution of 12 km, and a vertical  
141 resolution of 42 terrain-following layers covering the region from 20°N to southeast Alaska (60°N), and from the coast  
142 to 3000 km offshore (Figure S2). The physical and biogeochemical parameters are those described in Renault et al.  
143 (2021) and Deutsch et al. (2021), respectively. A complete description of the forcing and boundary conditions for the  
144 hindcast and future simulation is provided in Howard et al. (2020a) (see their Table 1).

### 145 2.3.1 | Model evaluation

146 Previous work with the 12 km model simulations described above, and comparison with a set of closely related  
147 higher resolution (4 km) simulations, has shown that the 12 km simulation successfully captures key climate responses  
148 (Howard et al., 2020b). The model also accurately reproduces the annual mean World Ocean Atlas 2018 (WOA18)  
149 temperature and oxygen distributions (Garcia et al., 2018; Locarnini et al., 2018) in the region of the California Cur-  
150 rent System (Deutsch et al., 2021; Howard et al., 2020b; Renault et al., 2021). Since the Pacific halibut surveys used  
151 in this study were conducted in summer (typically, June, July and August), we extended the previous evaluation to  
152 specifically assess model skill in resolving the summer climatology of oxygen and temperature distributions (Figures 2  
153 and S3). We also extended our quantitative evaluation of the model performance to include the region off southeast  
154 Alaska. To evaluate the model, we used climatological summer oxygen and temperature fields from the WOA18, as  
155 well as oxygen and temperature profile data from the World Ocean Database 2018 (Boyer, 2018) to evaluate the

156 simulated vertical structure (Figure S4).

157 In general, we found that the model effectively captures the observed large-scale summer features of temperature  
 158 and oxygen across our study domain (Figure 2). At 100 m, the model agrees well with the observed large-scale North-  
 159 South temperature gradient over the fisheries subareas 2A, 2B and 2C (Figure 2a-c). In the nearshore region (within  
 160 100 km from the coast), the simulated temperature in our region of interest between 35 and 58°N agrees exceptionally  
 161 well with the observations, with a mean temperature difference for the summer climatology of only 0.02°C. At 200  
 162 and 300 m, the model produces slightly colder waters than observed in the nearshore, but this difference is less than  
 163 0.4°C across all three subareas (Figure S3), and only 0.2°C for subarea 2C (between ~ 54 and 58°N).

164 The overall simulated oxygen and temperature vertical structure is consistent with the observations (Figure S4).  
 165 However, the model tends to underestimate the observed oxygen concentration on average (Figure S3b), with the  
 166 largest discrepancies (up to 35  $\mu\text{mol L}^{-1}$ ) at 100 m within 100 km from the coast. At 200 and 300 m, the bias between  
 167 the model and the observations is smaller (28 and 19  $\mu\text{mol L}^{-1}$ , respectively), and the simulated spatial pattern is  
 168 consistent with the observations. Some of these discrepancies might stem from the scarcity of summer observations  
 169 used to generate the World Ocean Atlas climatology, particularly in the region off Haida Gwaii and Prince of Wales  
 170 Island (See inset in Figure S4a). Additionally, this negative bias may be the result of previously identified mismatches  
 171 between modeled and observed density fields stemming from the boundary conditions (Deutsch et al., 2021; Howard  
 172 et al., 2020b; Renault et al., 2021).

## 173 2.4 | Definition of suitable aerobic habitat

174 As an indicator of Pacific halibut-specific suitable aerobic habitat, we used a recently revised Metabolic Index ( $\Phi$ ;  
 175 (Deutsch et al., 2015, 2020), which estimates the ratio of ambient oxygen supply ( $O_{2, \text{supply}}$ ) to Pacific halibut  $O_2$   
 176 demand ( $O_{2, \text{demand}}$ ) at a resting metabolic rate:

$$\Phi = \frac{O_{2, \text{supply}}}{O_{2, \text{demand}}} = A_0 \frac{pO_2}{\exp(-E_0/k_B(\frac{1}{T} - \frac{1}{T_{\text{ref}}}))} \quad (1)$$

177 This index is calculated based on ambient temperature ( $T$ , °K) and oxygen partial pressure ( $pO_2$ ,  $\text{atm}^{-1}$ ), the Boltz-  
 178 mann constant ( $k_B$ , eV), as well as ecophysiological parameters: the hypoxia tolerance ( $A_0$ ,  $\text{atm}^{-1}$ ) that applies at a  
 179 reference temperature ( $T_{\text{ref}} = 15^\circ\text{C}$ ), and the temperature sensitivity to hypoxia tolerance ( $E_0$ , eV). For the habitat to  
 180 be aerobically viable, the  $O_{2, \text{supply}}$  must at least meet the  $O_{2, \text{demand}}$  of a species. This condition restricts organisms  
 181 to waters with a  $pO_2$  above a minimum critical value. For resting metabolism, this threshold is typically measured  
 182 via laboratory respirometry (an extensive summary of respirometry studies is provided in Deutsch et al. (2020)). For  
 183 active metabolism required to sustain a population, the temperature-dependent minimum  $pO_2$  can be estimated as  
 184 that which bounds the geographic range of a species (Howard et al., 2020b). The resulting parameters yield a  $\Phi$  scale  
 185 that is normalized to an active ecological threshold (often denoted  $\Phi_{\text{crit}}$ ; (Deutsch et al., 2015, 2020; Howard et al.,  
 186 2020b) rather than the physiological threshold of laboratory conditions.

187 To estimate the active and temperature-dependent hypoxia tolerance of Pacific halibut, we considered the ob-  
 188 served  $T$  and  $O_2$  conditions in those locations with occurrences of Pacific halibut (sampled concurrently, see Section  
 189 2.2) over the full IPHC monitoring region (Figure 3a). Projecting species occurrences across the range of joint tem-  
 190 perature and  $pO_2$  conditions reveals that the lowest  $pO_2$  inhabited by Pacific halibut is dependent on temperature,  
 191 an observation common to most species (Deutsch et al., 2020). The parameters of  $\Phi$  (i.e.,  $A_0$  and  $E_0$  from Eqn. 1) are

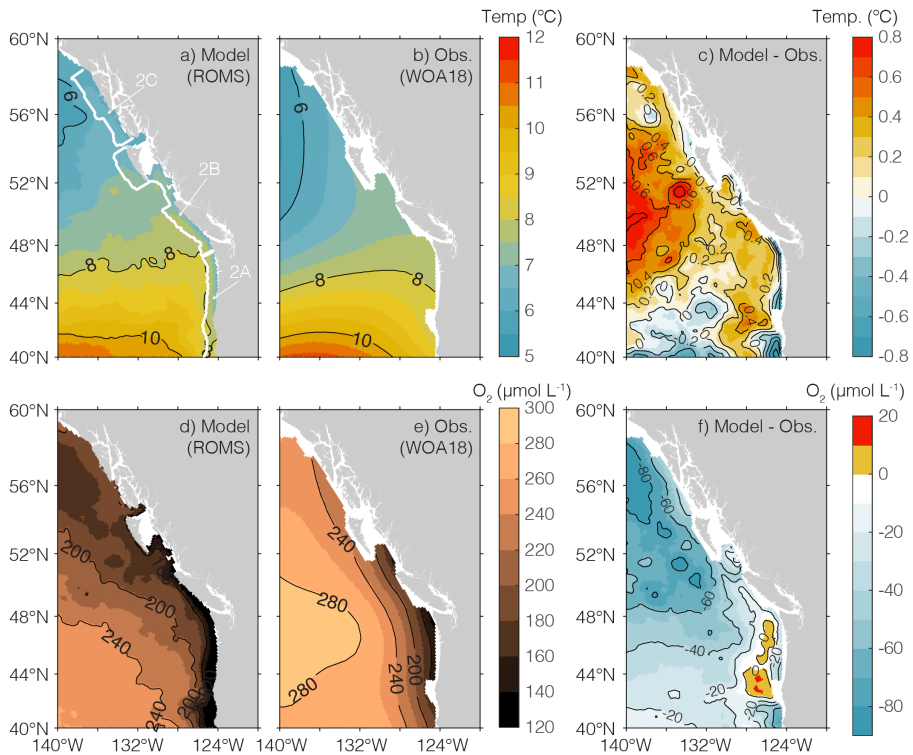


**FIGURE 2** Climatological summer (June-July-August) temperature (a-c) and oxygen (d-f) at 100 m depth, where Pacific halibut is abundant. The left panels show the model derived summer climatology (1994-2007). The middle panels show the summer climatology from the World Ocean Atlas (WOA18) re-gridded to the 12 km ROMS resolution. The difference (model minus observations) is shown in the right column. The white line on panel a) is the 100 km nearshore region for each IPHC subarea (2A, 2B, and 2C) used in the statistical analyses of Figure S3.

192 those which optimally delineate the inhabited and uninhabited regions in the state-space of temperature and  $pO_2$   
 193 (dashed line in Figure 3b), such that the realized niche has  $\Phi > 1$  while conditions with no species occurrences have  $\Phi$   
 194  $< 1$ . When fitting the model, the optimal parameters are chosen to maximize the F-score of the habitat categorization  
 195 (Deutsch et al., 2020; Shawe-Taylor and Cristianini, 2004).

196 Once all the ecophysiological parameters were derived,  $\Phi$  was estimated based on the summer mean temperature  
 197 and oxygen from the present and future simulations described in Section 2.3. The distribution of the estimated values  
 198 is similar between the ROMS-derived  $\Phi$  (calculated for the period 1998 - 2007) and observation-derived  $\Phi$  (calcu-  
 199 lated for the period 2009-2020) (Figure S5). This agreement provides further reassurance that, despite the moderate  
 200 simulated underestimation of oxygen concentration in the water column (e.g., Figure 2f), the model performs well  
 201 when translating the temperature and oxygen concentrations from the benthic habitat to the ecologically-relevant  
 202 metabolic index.

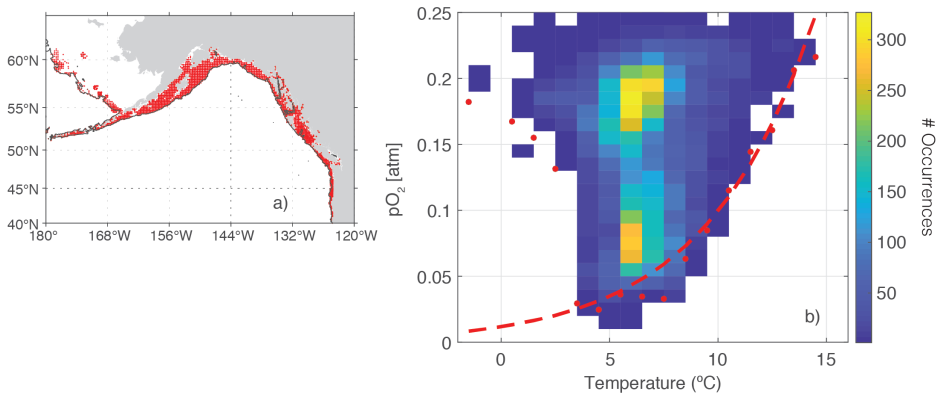


**FIGURE 3** a) Full geographical range of the IPHC Fishery Independent Setline Survey stations with near ocean floor temperature and oxygen measurements. b) temperature and oxygen partial pressure state-space at the locations shown in a) where Pacific halibut was present. The lowest  $pO_2$  associated to a given temperature class is indicated in red dots. The fitted model used to derive the  $\Phi$  ecophysiological parameters ( $A_0 = 3.65 \text{ atm}^{-1}$  and  $E_0 = 1.42 \text{ eV}$ ) is shown in dashed-red.

## 203 3 | RESULTS

### 204 3.1 | Regional oceanography and spatial Pacific halibut distribution

#### 205 3.1.1 | Summer oxygen, temperature and $\Phi$

206 To a large extent, coastal upwelling and downwelling define the oxygen and temperature features of the west coast  
 207 of the United States and Canada (Ware and McFarlane, 1989). In the southern subareas (2A and 2B, Figure 1), off  
 208 California, Oregon, Washington, and southern British Columbia, summer upwelling brings cold, low oxygen subsurface  
 209 water with subtropical influence to shallower depths (Adams et al., 2013; Ianson et al., 2003). Further north off  
 210 southeast Alaska (subarea 2C), coastal downwelling of subarctic water is persistent throughout the year, although  
 211 weaker in the summer months (Ware and McFarlane, 1989). The spatial pattern of northern downwelling and southern  
 212 upwelling in our study region partially contributes to latitudinal gradients in oxygen and temperature. In summer,  
 213 temperature at 100 m generally decreases northward from 8.2 °C in subarea 2A to 6.5 °C in subarea 2C (spatial mean  
 214 of the 100 km nearest to the coast for each subarea), while oxygen increases from 140  $\mu\text{mol L}^{-1}$  to 245  $\mu\text{mol L}^{-1}$   
 215 (Figure 2b,e). This latitudinal gradient is also apparent (although weaker) at 200 m and 300 m (not shown), and is  
 216 reflected in an overall northward increase in  $\Phi$  (Figure S6a,d,g), which is mainly driven by the spatial distribution of  
 217 oxygen. At 100 m, the difference between subarea 2A and 2C is notable, with a mean  $\Phi$  of 1.4 and 2.9 in the nearshore  
 218 waters of subareas 2A and 2C, respectively. As with oxygen, the latitudinal  $\Phi$  gradient becomes weaker with depth;  
 219 at 300 m, in the northern subarea (2C)  $\Phi$  is only 0.4 units higher than the value in the southern subarea 2A.

220 Water properties at the deepest layer of the water column (i.e., benthic habitat), where Pacific halibut tend  
 221 to be found, are shown in Figure 4. Temperatures above the 5th percentile ( $p_5$ ) of the Pacific halibut distribution  
 222 (3.7 °C) occur over most of the domain, from California to southeast Alaska. Oxygen above the  $p_5$  (a concentration  
 223 of 63  $\mu\text{mol L}^{-1}$  or  $O_2$  partial pressure of 0.04 atm) is more prevalent across the northern region of the domain (Fig-  
 224 ure 4b). South of 45 °N, ocean bottom oxygen concentrations in summer are lower. As in the water column (Figure  
 225 2), ocean bottom temperature decreases and oxygen increases northwards, with the exception of shallow (< 100 m),



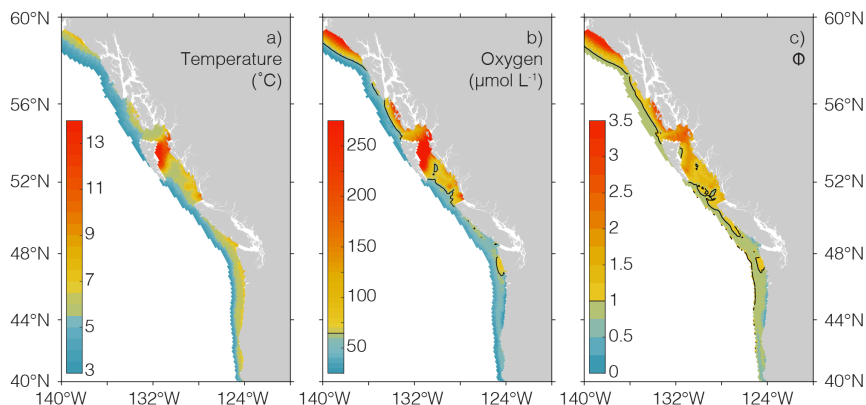


**FIGURE 4** ROMS-based mean (1994-2007) summer (June-August) ocean bottom temperature (a), Oxygen (b) and Metabolic index,  $\Phi$  (c). The contours in b) and c) indicate the value above which 95% of the Pacific halibut sampled at the FISS was found. i.e., the 5<sup>th</sup> percentile (p5). The p5 is 63  $\mu\text{mol L}^{-1}$  ( $\text{pO}_2$  of 0.04 atm at the p5 temperature and salinity) for dissolved oxygen, and 1.05 for  $\Phi$ . Properties are shown for bathymetry shallower than 1000 m.

226 semi-enclosed Hecate Strait (Figure 1), where temperature is approximately 10 °C higher than the surrounding ocean  
 227 bottom waters. In this shallow water column, strong tidal mixing (Perry et al., 1983) allows oxygenation so that oxygen  
 228 values are similar to those near the surface (> 200  $\mu\text{mol L}^{-1}$ ; Figure 4b). In the coastal region north of 45 °N, lower  
 229 temperatures and higher oxygen results in viable habitat for Pacific halibut, as demonstrated by the ocean bottom  $\Phi$   
 230 values higher than the  $\Phi_{crit}$  value of 1 (Figure 4c).

### 231 3.1.2 | Pacific halibut distribution

232 Pacific halibut in the O32 size class (i.e., individuals with fork length equal to or greater than 32 inches) concentrate  
 233 in the depth range of 100 – 300 m (Figure S7a) along the west coast of Oregon, Washington, British Columbia, and  
 234 southeast Alaska (Figure 5a). Within this depth range, the overall mean Pacific halibut CPUE (for subareas 2A, 2B  
 235 and 2C) is 4.7 ind./skate. By comparison, the mean CPUE of O32 Pacific halibut at depths shallower than 100 m or  
 236 deeper than 300 m is 2.9 ind./skate and 2.7 ind./skate, respectively. Smaller (U32) Pacific halibut (likely representing  
 237 younger fish) were found in shallower waters concentrated in the range from 0 to 200 m depth (Figure 5b and S6b),  
 238 with a mean of 3.2 ind./skate. The mean U32 CPUE below 200 m was lower, 1.5 ind./skate.

239 Regionally, the CPUE for both size classes of Pacific halibut are highest in the IPHC subarea 2C, with an overall  
 240 mean of 6.7 ind./skate (O32) across all depths. Within this subarea, there is an apparent region of higher Pacific halibut  
 241 density in the oceanic region off Prince of Wales Island and extending to Dixon Entrance (Figure 5a, see Figure 1 for  
 242 annotations). Intermediate CPUE values were found in subarea 2B off British Columbia, with an overall mean O32  
 243 of 3.7 ind./skate. In this region, O32 and U32 Pacific halibut appear to concentrate in Queen Charlotte Sound and  
 244 Hecate Strait (the region between Haida Gwaii and the northern tip of Vancouver Island, Figure 1). The lowest Pacific  
 245 halibut CPUE were found off Oregon and Washington in subarea 2A (overall O32 mean of 1.5 ind./skate).

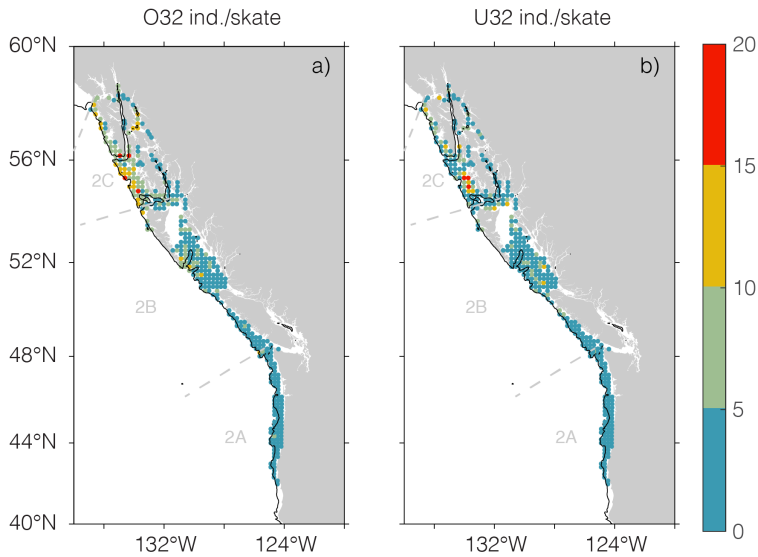


**FIGURE 5** Summer average (1998 – 2020) distribution of a) O32 and b) U32 Pacific halibut across the IPHC survey stations. Each data point represents a time series station. The black contour denotes 300 m bathymetry. IPHC subareas are indicated.

### 246 3.1.3 | Pacific halibut distribution and $\Phi$

247 We used fisheries data and space and time co-located model output to examine the relationship between Pacific  
 248 halibut CPUE, temperature,  $O_2$  concentrations, and  $\Phi$ . We segregated the Pacific halibut CPUE into model-based  $\Phi$   
 249 bins of 0.5, and calculated the mean CPUE for each group (Figure 6a,b). From this analysis, we found that the U32  
 250 and O32 size classes are related with oxygen, temperature, and  $\Phi$  to varying degrees. The maximum O32 CPUE was  
 251 found in waters with  $\Phi$  values higher than 1.5, where the mean CPUE at the 1.5-2  $\Phi$  class was  $7.1 \pm 6.6$  ind./skate.  
 252 For U32, the maximum values were found in water with higher  $\Phi$  (2.5 – 4), with a mean CPUE of  $8.9 \pm 6.4$  ind./skate.  
 253 The higher  $\Phi$  associated with maximum U32 values partially reflect the shallower depth preferences of these smaller  
 254 fish (Sadorus et al., 2014) (Figure S7b).

255 Results similar to those presented above were obtained from an analysis with observed environmental data sam-  
 256 pled concurrently with the Pacific halibut but conducted over a different period (2009-2020; see Section 2.2 and  
 257 Figure S5). As expected, the comparison of fisheries data with both model output and oceanographic observations  
 258 indicates a strong relationship between Pacific halibut and  $\Phi$  over the period between 1998 – 2020.

### 259 3.2 | Temporal variability in habitat distribution and CPUE of Pacific halibut

260 We did not identify any significant long-term regional trend in mean Pacific halibut CPUE over the period 1998-2020  
 261 (not shown). However, interannual variability in O32 was observed in subarea 2C (Figure 7a), with two periods of time  
 262 with elevated O32 CPUE (1.5-2 ind./skate above the long-term mean) over the years 2000-2005 and 2012-2019. This  
 263 interannual variability in O32 Pacific halibut was correlated with the Pacific Decadal Oscillation (PDO;  $r = 0.46$ ,  $p < 0.1$ ).

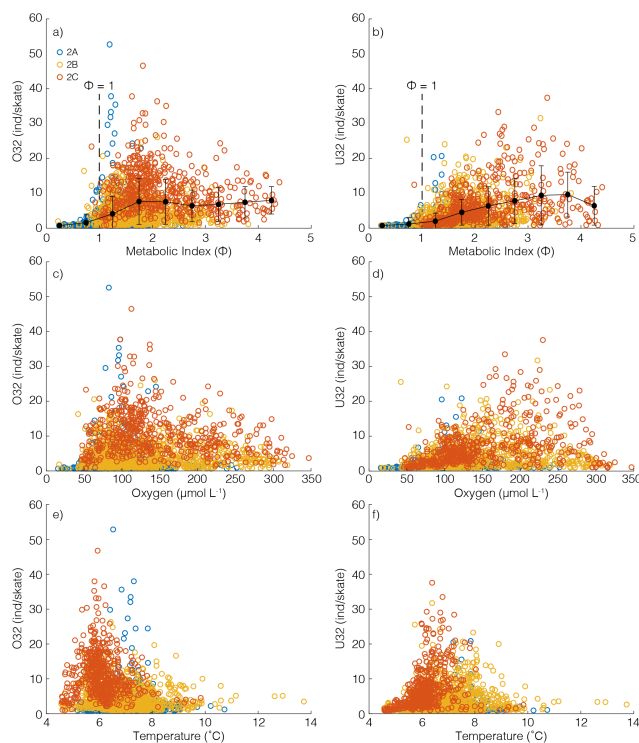


**FIGURE 6** Relationship between model-derived  $\Phi$  (top row), oxygen (middle row), and temperature (bottom row), and Pacific halibut over 32 inches (O32; left column) and under 32 inches (U32; right column). Oxygen, temperature, and  $\Phi$  were extracted based on the date (month and year), depth, and geographic location of the Pacific halibut survey samples over the period 1998-2007. The black points and trend line in a) and b) indicate the mean and standard deviation in Pacific halibut CPUE for each 0.5  $\Phi$  class. The vertical dashed lines indicate the  $\Phi_{crit} = 1$ , which represents the minimum value necessary for active metabolism (see section 2.4).

264 During the Pacific halibut survey (1998-2020), the PDO was predominantly negative (Figure 7), with the exception  
 265 of two positive episodes: around year 2004 and more recently between 2014 and 2017. These two instances of  
 266 positive PDO roughly correspond to the period of higher O32 Pacific halibut CPUE observed in 2C. In contrast, no  
 267 statistically-significant relationship between Pacific halibut CPUE and PDO was apparent in more southern subareas  
 268 2A or 2B, where Pacific halibut CPUE was overall lower. Similarly, there was no significant relationship between PDO  
 269 and U32 CPUE in any subarea analysed (Figure S8).

270 The model simulation was able to accurately reproduce interannual shifts in surface oceanographic variables  
 271 related to the PDO (Figure S8). In subareas 2C and 2B, sea surface temperature tends to increase during the positive  
 272 PDO phase (Figure S8a), while surface water oxygen and  $\Phi$  tend to show negative anomalies (relative to the 1994-  
 273 2007 simulated climatology). The opposite is true over periods when the PDO was mainly negative (e.g., between  
 274 1997 to 2003). The correlation of environmental variables with the PDO index is restricted to the surface layer  
 275 (approximately top 50 m). In contrast, temperature, oxygen, and  $\Phi$  in the Pacific halibut habitat (near ocean bottom  
 276 waters) do not appear related to variations in the PDO ( $r = 0.04$ ; Figure 8).

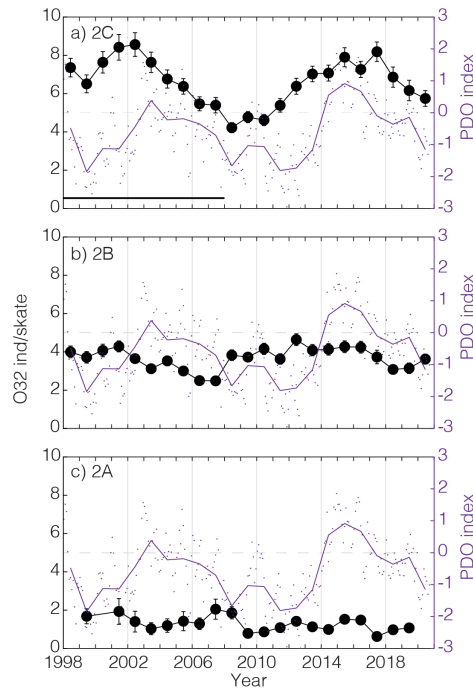


**FIGURE 7** Annual time series of mean O32 Pacific halibut in subareas a) 2C, b) 2B, and c) 2A. The error bars denote the standard error of the spatial mean. The annual mean PDO (solid line) and the monthly values (individual markers) are also shown (right hand axis). The horizontal black line in panel a) indicates the overlapping period between the fisheries observations (1998-2020) and the model simulation (1994-2007). The dashed horizontal grid line indicates a value of the PDO index of zero.

### 277 3.3 | Future projections

278 Model simulations provide the opportunity to explore future environmental scenarios and their potential impact on  
 279 Pacific halibut distributions. In RCP8.5 (high CO<sub>2</sub> emissions) simulations representing the end of the 21<sup>st</sup> century,  
 280 ocean bottom temperature increases by more than 1.5 °C along the coast and up to 3 °C in shallow regions such  
 281 as Hecate Strait (Figure 9c). This warming leads to a projected displacement of waters with Pacific halibut-favored  
 282 temperature (p50, 5.9 °C) further offshore to deeper depths (Figure 9b). Simulated oxygen concentration is projected  
 283 to decrease everywhere, and the area with ocean bottom O<sub>2</sub> concentrations above the O<sub>2,p5</sub> (63 μmol L<sup>-1</sup>) will be  
 284 reduced to a narrow coastal band in Queen Charlotte Sound, off Prince of Wales Island and in Hecate Strait (Figure  
 285 9e). This reduction in O<sub>2</sub> is the main driver of the overall decrease in ocean bottom  $\Phi$  projected for the end of the 21<sup>st</sup>  
 286 century, as can be seen in the similarity of the O<sub>2,p5</sub> and the  $\Phi = 1$  contours (Figure 9e,h). The area with suitable habitat  
 287 to sustain active metabolism of Pacific halibut ( $\Phi > 1$ ) is projected to disappear everywhere south of Vancouver Island.  
 288 This change translates into approximately a five degrees latitude northward retreat of the southernmost boundary of  
 289 Pacific halibut suitable habitat. Further north, suitable habitat will be restricted to the coastal region off Hecate Strait  
 290 and Prince of Wales Island.

291 To determine future changes in the extent of Pacific halibut habitat, we analyzed the change in the volume of

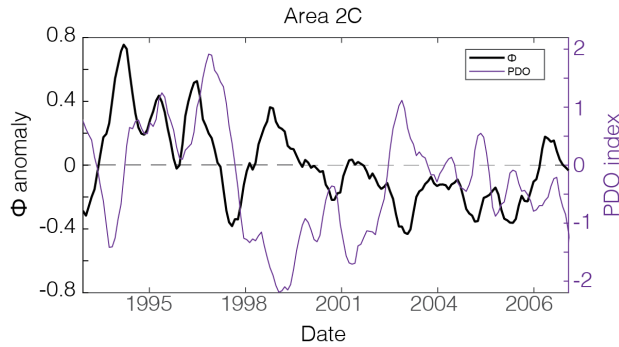


**FIGURE 8** Time series of model-based bottom water  $\Phi$  anomalies for the subarea 2C for the period of the model simulation (indicated in Figure 7a). The PDO index is shown in the right axis, with the horizontal dashed line indicating a PDO index of zero. The time series were averaged spatially over a region delineated by the 300 m isobath. Both time series were smoothed using a 6-months moving average.

292 bottom waters with different  $\Phi$  values. For this analysis, we focused on the bottom layer of the model above the  
 293 ocean floor, in a region delimited by the 300 m isobath for each IPHC subarea considered (Figure 10). We found that  
 294 the volume of water below the  $\Phi_{crit}$  ( $\Phi = 1$ ) in summer will at least double by year 2100, considerably limiting the  
 295 potential habitat for Pacific halibut in the future in subareas 2B and 2C. In subarea 2B off British Columbia, unsuitable  
 296 habitat will occupy approximately 90% of the layer above the sediments around the year 2100, as compared to 40%  
 297 in the present day. Further north (subarea 2C) projected impacts are similar, with 80% of the benthic habitat below  
 298 the  $\Phi_{crit}$  by year 2100, as compared to only 20% at present. These results strongly suggest a potential future shift in  
 299 Pacific halibut distribution to the northern range of our study region.

## 300 4 | DISCUSSION

301 Given the commercial importance of the Pacific halibut fishery, changes in the abundance and distribution of this  
 302 benthic species will have significant economic consequences. By combining fisheries surveys of Pacific halibut with  
 303 oceanographic data and output from an ocean biogeochemical model, we examined the potential impacts of deoxy-  
 304 genation and ocean warming on habitat availability for Pacific halibut. Our results show a clear spatial coherence  
 305 between Pacific halibut and present-day oxygen, temperature and  $\Phi$  at the southernmost boundary of their distri-  
 306 bution range. Using model-based projections, we examined future potential contraction of preferred habitat, and  
 307 assessed how the spatial distribution of Pacific halibut would change.

### 308 4.1 | Spatial and temporal variability

309 The time series of spatially-resolved and fisheries-independent IPHC Pacific halibut CPUE allow us to examine tem-  
 310 poral and spatial relationships between the distribution of Pacific halibut and ocean bottom oxygen and temperature.  
 311 Based on an analysis of more than two decades of observations, our results demonstrate a strong spatial relationship  
 312 between Pacific halibut CPUE,  $O_2$ , and derived  $\Phi$  values (Figure 6). These results agree with the previous work of  
 313 Sadorus et al. (2014), who examined a shorter time series (2006 – 2009), and found that dissolved oxygen, and to a

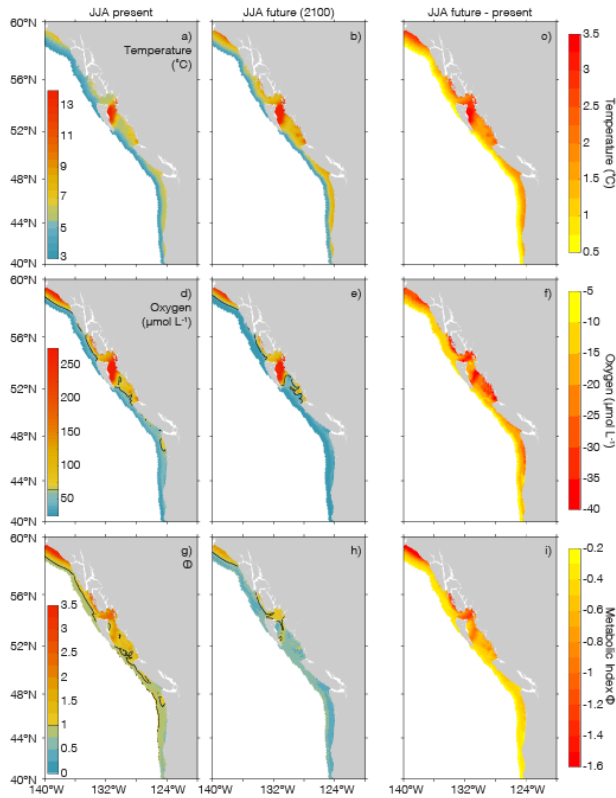


**FIGURE 9** Ocean bottom temperature (top row), oxygen (middle row) and  $\Phi$  (bottom row) for the summer mean over 1994-2007 (left column), future projection centered around year 2100 (middle column), and future change (future - present). The contours indicate the p5 for oxygen ( $63 \mu\text{mol L}^{-1}$  or a  $p\text{O}_2$  of 0.04 atm at the p5 conditions of temperature and salinity) and  $\Phi$  (1.05). The figures in the left column are the same as those in Figure 4.

314 lesser extent temperature, are key variables explaining Pacific halibut distribution off the US west coast and Southern  
 315 British Columbia.

316 Our analysis of individual sampling stations and aggregated IPHC subareas indicate that there has been no sig-  
 317 nificant trend in Pacific halibut CPUE in our study zone over the period 1998-2020. However, there is apparent co-  
 318 variability between the PDO and mean regional summer O32 abundance in subarea 2C (Figure 7a). This relationship is  
 319 sustained, although weaker (Pearson = 0.33) when O32 biomass (lbs/skate; not shown), rather than O32 abundance  
 320 (ind./skate), is considered. Relationships between Pacific halibut growth and recruitment and North Pacific climatic  
 321 variability have been observed previously (Clark et al., 1999; Hare and Mantua, 2000; Hollowed et al., 2001; Lehodey  
 322 et al., 2006; Yati et al., 2020). The analysis of Chhak and Di Lorenzo (2007) (as seen in Franks et al. (2013)) suggests  
 323 that positive phases of the PDO (driven by a stronger and southward-displaced Aleutian low) are typically related to  
 324 stronger downwelling conditions in the coastal Alaskan Gyre (e.g., in southeast Alaska, subarea 2C). In agreement with  
 325 this result, we found a positive relationship between the PDO and model-based surface temperature: both are higher  
 326 in the periods when the O32 abundance is elevated. Higher surface temperature leads to a reduction in  $\text{O}_2$  solubility,  
 327 which we observe as a negative surface  $\text{O}_2$  and  $\Phi$  anomaly in those periods of time where the PDO is positive (Figure

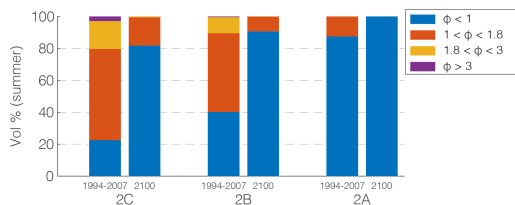


**FIGURE 10** Volume fraction of several  $\Phi$  classes in the deepest layer at each IPHC subarea (spatial distribution shown in Figure 9g,h), delimited by the 300 m isobath for the summer season. For each subarea, the summer climatology of years 1994-2007 is shown in the left column, and summer means of the future projection centered around year 2100 on the right.

328 S9).

329 Whereas the PDO is largely expressed in surface ocean waters, Pacific halibut will respond more directly to  
 330 ocean conditions in their benthic habitat (Sadorus et al., 2014). However, we found that the relationship between  
 331 PDO, temperature,  $O_2$ , and  $\Phi$  observed at the surface is absent in the benthic habitat (Figure 8). Ocean bottom water  
 332 properties seem particularly decoupled from the PDO index over the strong El Niño period from 1997-1998, with  
 333 higher than usual temperature,  $O_2$ , and  $\Phi$ , and a positive value of the PDO and the Oceanic Niño Index (ONI). El Niño is  
 334 associated with stronger downwelling, indicating a potential interplay of subtropical and subarctic signals (Hollowed  
 335 et al., 2001). This result suggests that the link between Pacific halibut abundance and the PDO index in subarea 2C  
 336 reflects indirect mechanisms coupling surface and bottom waters, rather than changes in bottom water temperature,  
 337  $O_2$  or  $\Phi$ , per se.

338 Changes in mixed layer primary productivity could be a potential mechanism coupling surface water and benthic  
 339 habitat, with higher productivity driving greater carbon export and higher benthic oxygen demand. To address this  
 340 possibility, we used satellite-based time series of surface water chlorophyll concentrations as a proxy for phytoplank-  
 341 ton biomass across our survey regions (not shown). This analysis did not reveal any clear relationship between surface  
 342 chlorophyll and bottom water oxygen,  $\Phi$  or Pacific halibut abundance. We are thus unable to provide a mechanistic  
 343 explanation linking the PDO and halibut abundance. We note, however, that recent work has suggested that the  
 344 coupling of the PDO with ecosystem processes has become weaker in recent years due to an overall weakening of  
 345 the Aleutian low (Litzow et al., 2020).

## 346 4.2 | Future habitat availability

347 The spatial distribution of Pacific halibut is consistent with a spatial pattern of increasing ocean bottom oxygen and  
 348  $\Phi$  from south to north in our study region. Based on the present day ecological  $\Phi_{crit}$  distribution ( $\Phi = 1$ ), we were  
 349 able to estimate future changes in suitable Pacific halibut habitat by the end of the century under a business-as-usual  
 350  $CO_2$  emissions scenario. Under this scenario, it is projected that suitable Pacific halibut habitat will be restricted to  
 351 the coastal region off Prince of Wales Island in subarea 2C by the end of the 21st century (Figure 9h). This habitat  
 352 contraction is related to a projected decrease in bottom water oxygen and  $\Phi$ .

353 In the California Current System, a combination of increased upwelling-favorable winds in spring, and increased  
 354 stratification in summer are the main mechanisms for the strong oxygen decline, which drives much of the decrease in  
 355  $\Phi$  (Howard et al., 2020a). Specifically, Howard et al. (2020b) attribute between 30 to 50% of the change to a decrease

356 in O<sub>2</sub> solubility in source waters, and the rest of the change to an increase in apparent oxygen utilization. A recent  
357 study by Dussin et al. (2019) found that combined changes in the nutrient and oxygen content of source waters might  
358 have a greater impact in the enhanced deoxygenation in the California Current than changes in upwelling winds alone.

359 Results from the future high CO<sub>2</sub> emissions simulation show that by the end of this century, the largest changes  
360 in temperature, oxygen and  $\Phi$  are projected in subareas 2C and 2B at depths near 100 m (Figure S6), where Pacific  
361 halibut abundance is greatest (Figure S7). This change could have a disproportionate impact on the habitat environ-  
362 ment of younger Pacific halibut (U32), which tend to live at shallower depths (Figure S7b), potentially pushing this size  
363 class towards more favorable regions either northward or nearer to the coast, following the general trend of other  
364 species around the globe (Sumaila et al. (2011), and references therein). It has been suggested, however, that Pacific  
365 halibut might exhibit a lateral, rather than vertical, redistribution in response to hypoxia events (Sadorus et al., 2014),  
366 supporting the idea of a northward migration. The waters of Hecate Strait (embedded in subarea 2B) are of partic-  
367 ular interest, as a shallow region recognized as an important Pacific halibut spawning and nursery region (Loher and  
368 Wischniowski, 2008). Most of the Pacific halibut eggs spawned in this zone tend to settle there (Carpi et al., 2021),  
369 creating an important source of Pacific halibut for the local economy. This region will experience the most dramatic  
370 changes in the benthic habitat (Figure 9), with potential, but unknown repercussions for the regional Pacific halibut  
371 life cycle.

372 In the southernmost subarea (2A), low  $\Phi$  values are already present near the coast due to summer upwelling. As  
373 a consequence, this region is projected to experience a less drastic change in  $\Phi$  in comparison with subareas 2B and  
374 2C. Instead, low values are projected to extend further offshore (Figure S6). Despite the small absolute change in  $\Phi$   
375 values by the end of the century in subarea 2A, future deoxygenation will potentially lead to the complete absence  
376 of suitable habitat for Pacific halibut in the US states of Washington and Oregon, limiting the US fishery to the state  
377 of Alaska. This potential habitat redistribution is in line with previous findings suggesting that climate change might  
378 lead to an increase in catch potential in the Arctic and subarctic regions (Cheung et al., 2010; Sumaila et al., 2011).

379 Given that a large percentage of the commercially-exploited marine species are shared between neighboring  
380 countries (Palacios-Abrantes et al., 2020), the potential shift in suitable Pacific halibut habitat to the north of the  
381 U.S.-Canada border might drive important economical (e.g., commercial and recreational fisheries) and societal (e.g.,  
382 subsistence fishery) consequences for the Pacific halibut fisheries (Sumaila and VanderZwaag, 2020). Due to the  
383 projected northward displacement of suitable habitat, the potential positive impact on Pacific halibut fisheries off  
384 Alaska might be offset by other factors, e.g., reduced price due to the smaller size typically observed under higher  
385 temperatures, or a protein substitution (Sumaila et al., 2011). To precisely identify the economic impact, future studies  
386 could model the impact at a local level through integration of biophysical changes, fish population dynamics, and  
387 fisheries economics. Since Pacific halibut is a transboundary fish that migrates between the Exclusive Economic Zones  
388 of Canada (IPHC subarea 2B) and the U.S. (IPHC subareas 2A and 2C), the two countries co-manage the fish stock  
389 via the IPHC. The exact valuation of the shift in the fish distribution due to climate change can be a critical standard  
390 in addressing potential conflicts in co-management.

### 391 4.3 | Caveats

392 In interpreting our results, it is important to consider a number of complicating factors. Our simulations of habitat  
393 contraction are based solely on the present-day relationship between Pacific halibut abundance and oceanographic  
394 conditions, derived from a 17-year time series. However, other factors not considered in the future projections might  
395 play a role in defining the habitat of groundfish species. For example, Youcef et al. (2015) found that the potential  
396 negative impact of a reduction in oxygen concentration on Greenland halibut in the Gulf of St. Lawrence was compen-



sated by other factors such as food abundance, food availability, and/or predator density. It is possible, even likely, that similar mechanisms complicate the observed relationship between PDO and O32 in subarea 2C (and potentially explain why this relationship was not observed in other subareas). We also note that the domain of our future projection does not resolve temperature and oxygen changes in some coastal regions off British Columbia and other fjords in Southeast Alaska, where Pacific halibut abundance is low. Unknown future changes in habitat availability could exacerbate this trend, or open new habitat regions for Pacific halibut. Given the large degree of interconnectivity of Pacific halibut in the Northeast Pacific (Sadorus et al., 2021), future studies on climate change impacts would benefit from considering the full range of Pacific halibut distribution, for example by utilizing a high-resolution global earth system model. Continued sampling of oceanographic and fisheries-independent Pacific halibut abundance data will extend the observation-based time series of environmental variables, and contribute to a better understanding of the relationship between Pacific halibut interannual variability and oceanographic properties.

Finally, it is important to note that our future model projection is based on only one model and one potential future scenario (RCP8.5). Alternative scenarios have been shown to generate significant differences in the projected future distributions of several groundfish in the Eastern Bering Sea (Rooper et al., 2020). The actual impacts of future ocean warming and deoxygenation on Pacific halibut and other fisheries abundance will thus depend directly on the approaches used to curb global greenhouse gas emissions, harvest regulations, as well as climate change adaptation policies (Sumaila et al., 2019).

## 5 | CONCLUSIONS

Using a combination of observations and model simulations, we derive an index of Pacific halibut habitat suitability for active metabolism ( $\Phi$ ) based on the relationship between environmental oxygen supply and biogeographically-derived ecophysiological traits. By including information from a decadal time series of Pacific halibut CPUE, we show that interannual variability in Pacific halibut CPUE in the northernmost region (off Prince of Wales Island) may be coherent with the Pacific Decadal Oscillation. In contrast, the PDO shows no significant association with the near ocean bottom  $\Phi$ , suggesting that the PDO relationship with Pacific halibut CPUE might reflect an indirect coupling. Future projections of ocean deoxygenation and warming are expected to lead to a reduction in suitable habitat for Pacific halibut, particularly in the southernmost region analyzed here (subarea 2A). A shift of approximately five degrees northward of suitable habitat will likely lead to a northward displacement of Pacific halibut populations. Further work with bioeconomic models might unveil potentially strong implications for ecosystems and fisheries.

## Acknowledgements

A.C.F and P.D.T acknowledge support from the Natural Sciences and Engineering Research Council of Canada, and from the MEOPAR project OxyNet: A network to examine ocean deoxygenation trends and impacts

## references

- Adams, K. A., Barth, J. A. and Chan, F. (2013) Temporal variability of near-bottom dissolved oxygen during upwelling off central Oregon. *Journal of Geophysical Research: Oceans*, **118**, 4839–4854.
- Bianucci, L., Fennel, K., Chabot, D., Shackell, N. and Lavoie, D. (2015) Ocean biogeochemical models as management tools: a case study for Atlantic wolffish and declining oxygen. *ICES Journal of Marine Science*, **73**, 263–274.

- 433 Boyer, T.P., O. B. C. C. H. G. A. G. R. L. A. M. C. P. J. R. D. S. I. S. K. W. M. Z. (2018) World Ocean Database 2018. NOAA Atlas  
434 NESDIS, 75, 27.
- 435 Breitburg, D., Levin, L. A., Oschlies, A., Grégoire, M., Chavez, F. P., Conley, D. J., Garçon, V., Gilbert, D., Gutiérrez, D., Isensee,  
436 K., Jacinto, G. S., Limburg, K. E., Montes, I., Naqvi, S. W. A., Pitcher, G. C., Rabalais, N. N., Roman, M. R., Rose, K. A., Seibel,  
437 B. A., Telszewski, M., Yasuhara, M. and Zhang, J. (2018) Declining oxygen in the global ocean and coastal waters. *Science*,  
438 359, eaam7240.
- 439 Campana, S. E., Stefánsdóttir, R. B., Jakobsdóttir, K. and Sólmundsson, J. (2020) Shifting fish distributions in warming sub-  
440 arctic oceans. *Scientific Reports*, 10, 16448.
- 441 Carpi, P., Loher, T., Sadorus, L. L., Forsberg, J. E., Webster, R. A., Planas, J. V., Jasonowicz, A., Stewart, I. J. and Hicks, A. C.  
442 (2021) Ontogenetic and spawning migration of Pacific halibut: a review. *Reviews in Fish Biology and Fisheries*, 31, 879–908.
- 443 Cheung, W. W., Lam, V. W., Sarmiento, J. L., Kearney, K., Watson, R. and Pauly, D. (2009) Projecting global marine biodiversity  
444 impacts under climate change scenarios. *Fish and Fisheries*, 10, 235–251.
- 445 Cheung, W. W. L., Lam, V. W. Y., Sarmiento, J. L., Kearney, K., Watson, R., Zeller, D. and Pauly, D. (2010) Large-scale re-  
446 distribution of maximum fisheries catch potential in the global ocean under climate change. *Global Change Biology*, 16,  
447 24–35.
- 448 Chhak, K. and Di Lorenzo, E. (2007) Decadal variations in the California Current upwelling cells. *Geophysical Research Letters*,  
449 34.
- 450 Christian, J. R. and Holmes, J. (2016) Changes in albacore tuna habitat in the northeast Pacific ocean under anthropogenic  
451 warming. *Fisheries Oceanography*, 25, 544–554.
- 452 Clark, W. G. and Hare, S. R. (2002) Effects of climate and stock size on recruitment and growth of Pacific halibut. *North*  
453 *American Journal of Fisheries Management*, 22, 852–862.
- 454 Clark, W. G., Hare, S. R., Parma, A. M., Sullivan, P. J. and Trumble, R. J. (1999) Decadal changes in growth and recruitment of  
455 Pacific halibut (*Hippoglossus stenolepis*). *Canadian Journal of Fisheries and Aquatic Sciences*, 56, 242–252.
- 456 Clarke, T. M., Reygondeau, G., Wabnitz, C., Robertson, R., Ixquiac-Cabrera, M., López, M., Ramírez Coghi, A. R., del Río Iglesias,  
457 J. L., Wehrtmann, I. and Cheung, W. W. (2021) Climate change impacts on living marine resources in the Eastern Tropical  
458 Pacific. *Diversity and Distributions*, 27, 65–81.
- 459 Collins, M., Knutti, R., Arblaster, J., Dufresne, J.-L., Fichetef, T., Friedlingstein, P., Gao, X., Gutowski, W. J., Johns, T., Krinner,  
460 G., Shongwe, M., Tebaldi, C., Weaver, A. J. and Wehner, M. (2013) Long-term Climate Change: Projections, Commitments  
461 and Irreversibility. *Climate Change 2013: The Physical Science Basis. Contribution of Working Group I to the Fifth Assessment*  
462 *Report of the Intergovernmental Panel on Climate Change*.
- 463 Deutsch, C., Ferrel, A., Seibel, B., Pörtner, H.-O. and Huey, R. B. (2015) Climate change tightens a metabolic constraint on  
464 marine habitats. *Science*, 348, 1132–1135.
- 465 Deutsch, C., Frenzel, H., McWilliams, J. C., Renault, L., Kessouri, F., Howard, E., Liang, J.-H., Bianchi, D. and Yang, S. (2021)  
466 Biogeochemical variability in the California Current System. *Progress in Oceanography*, 196, 102565.
- 467 Deutsch, C., Penn, J. L. and Seibel, B. (2020) Metabolic trait diversity shapes marine biogeography. *Nature*, 585, 557–562.
- 468 Dussin, R., Curchitser, E., Stock, C. and Van Oostende, N. (2019) Biogeochemical drivers of changing hypoxia in the California  
469 Current Ecosystem. *Deep Sea Research Part II: Topical Studies in Oceanography*, 169–170, 104590.
- 470 Francis, R. C. and Hare, S. R. (1994) Decadal-scale regime shifts in the large marine ecosystems of the North-east Pacific: a  
471 case for historical science. *Fisheries Oceanography*, 3, 279–291.

- 472 Franco, A. C., Ianson, D., Ross, T., Hamme, R. C., Monahan, A. H., Christian, J. R., Davelaar, M., Johnson, W. K., Miller, L. A.,  
473 Robert, M. and Tortell, P. D. (2021) Anthropogenic and climatic contributions to observed carbon system trends in the  
474 Northeast Pacific. *Global Biogeochemical Cycles*, **35**, e2020GB006829.
- 475 Franks, P. J., Lorenzo, E. D., Goebel, N. L., Chenillat, F., Rivière, P., Edwards, C. A. and Miller, A. J. (2013) Modeling physical-  
476 biological responses to climate change in the California Current System. *Oceanography*.
- 477 Garcia, H. E., Weathers, K., Paver, C. R., Smolyar, I., Boyer, T. P., Locarnini, R. A., Zweng, M. M., Mishonov, A. V., Baranova, O. K.,  
478 Seidov, D. and Reagan, J. R. (2018) World Ocean Atlas 2018. Volume 3: Dissolved Oxygen, Apparent Oxygen Utilization,  
479 and Oxygen Saturation. *A. Mishonov, Technical Ed.; NOAA Atlas NESDIS 83, 38pp.*
- 480 Gilly, W. F., Beman, J. M., Litvin, S. Y. and Robison, B. H. (2013) Oceanographic and biological effects of shoaling of the oxygen  
481 minimum zone. *Annual Review of Marine Science*, **5**, 393–420. PMID: 22809177.
- 482 Haigh, R., Ianson, D., Holt, C. A., Neate, H. E. and Edwards, A. M. (2015) Effects of ocean acidification on temperate coastal  
483 marine ecosystems and fisheries in the Northeast Pacific. *PLOS ONE*, **10**, 1–46.
- 484 Hare, S. R. and Mantua, N. J. (2000) Empirical evidence for north Pacific regime shifts in 1977 and 1989. *Progress in Oceanog-*  
485 *raphy*, **47**, 103–145.
- 486 Hollowed, A. B., Hare, S. R. and Wooster, W. S. (2001) Pacific Basin climate variability and patterns of Northeast Pacific marine  
487 fish production. *Progress in Oceanography*, **49**, 257–282. Pacific climate variability and marine ecosystem impacts.
- 488 Howard, E. M., Frenzel, H., Kessouri, F., Renault, L., Bianchi, D., McWilliams, J. C. and Deutsch, C. (2020a) Attributing causes  
489 of future climate change in the California Current System with multimodel downscaling. *Global Biogeochemical Cycles*, **34**,  
490 e2020GB006646.
- 491 Howard, E. M., Penn, J. L., Frenzel, H., Seibel, B. A., Bianchi, D., Renault, L., Kessouri, F., Sutula, M. A., McWilliams, J. C. and  
492 Deutsch, C. (2020b) Climate-driven aerobic habitat loss in the California Current System. *Science Advances*, **6**.
- 493 Howarth, R., Chan, F., Conley, D. J., Garnier, J., Doney, S. C., Marino, R. and Billen, G. (2011) Coupled biogeochemical cycles:  
494 eutrophication and hypoxia in temperate estuaries and coastal marine ecosystems. *Frontiers in Ecology and the Environment*,  
495 **9**, 18–26.
- 496 Ianson, D., Allen, S. E., Harris, S. L., Orians, K. J., Varela, D. E. and Wong, C. S. (2003) The inorganic carbon system in the  
497 coastal upwelling region west of Vancouver Island, Canada. *Deep Sea Research Part I: Oceanographic Research Papers*, **50**,  
498 1023 – 1042.
- 499 IPHC (2021) IPHC Fishery-Independent Setline Survey Sampling Manual, IPHC–2021–VSM01, 36 pp.
- 500 Keeling, R. F., Körtzinger, A. and Gruber, N. (2010) Ocean deoxygenation in a warming world. *Annual Review of Marine Science*,  
501 **2**, 199–229.
- 502 Kwon, E. Y., Deutsch, C., Xie, S.-P., Schmidtko, S. and Cho, Y.-K. (2016) The north Pacific oxygen uptake rates over the past  
503 half century. *Journal of Climate*, **29**, 61 – 76.
- 504 Lehodey, P., Alheit, J., Barange, M., Baumgartner, T., Beaugrand, G., Drinkwater, K., Fromentin, J.-M., Hare, S. R., Ottersen, G.,  
505 Perry, R. I., Roy, C., van der Lingen, C. D. and Werner, F. (2006) Climate variability, fish, and fisheries. *Journal of Climate*,  
506 **19**, 5009 – 5030.
- 507 Levin, L. A., Ekau, W., Gooday, A. J., Jorissen, F., Middelburg, J. J., Naqvi, S. W. A., Neira, C., Rabalais, N. N. and Zhang, J. (2009)  
508 Effects of natural and human-induced hypoxia on coastal benthos. *Biogeosciences*, **6**, 2063–2098.
- 509 Litzow, M. A., Hunsicker, M. E., Bond, N. A., Burke, B. J., Cunningham, C. J., Gosselin, J. L., Norton, E. L., Ward, E. J. and Zador,  
510 S. G. (2020) The changing physical and ecological meanings of North Pacific Ocean climate indices. *Proceedings of the*  
511 *National Academy of Sciences*, **117**, 7665–7671.

- 512 Locarnini, R. A., Mishonov, A. V., Baranova, O. K., Boyer, T. P., Zweng, M. M., Garcia, H. E., Reagan, J. R., Seidov, D., Weathers,  
513 K., Paver, C. R. and Smolyar, I. (2018) World Ocean Atlas 2018. Volume 1: Temperature. A. Mishonov, Technical Ed.; NOAA  
514 Atlas NESDIS 81, 52pp.
- 515 Loher, T. and Wischniowski, S. (2008) Using otolith chemistry to determine halibut nursery origin: progress in 2007. Int. Pac.  
516 Halibut Comm. report of assessment and research activities 2007:555-562.
- 517 Long, M. C., Deutsch, C. and Ito, T. (2016) Finding forced trends in oceanic oxygen. *Global Biogeochemical Cycles*, **30**, 381–397.
- 518 Mantua, N. J., Hare, S. R., Zhang, Y., Wallace, J. M. and Francis, R. C. (1997) A Pacific interdecadal climate oscillation with  
519 impacts on salmon production. *Bulletin of the American Meteorological Society*, **78**, 1069 – 1080.
- 520 Maunder, M. N., Sibert, J. R., Fonteneau, A., Hampton, J., Kleiber, P. and Harley, S. J. (2006) Interpreting catch per unit effort  
521 data to assess the status of individual stocks and communities. *ICES Journal of Marine Science*, **63**, 1373–1385.
- 522 McLean, M., Mouillot, D., Lindegren, M., Engelhard, G., Villéger, S., Marchal, P., Brind'Amour, A. and Auber, A. (2018) A climate-  
523 driven functional inversion of connected marine ecosystems. *Current Biology*, **28**, 3654–3660.e3.
- 524 Moore, J., Doney, S. C., Kleypas, J. A., Glover, D. M. and Fung, I. Y. (2001) An intermediate complexity marine ecosystem model  
525 for the global domain. *Deep Sea Research Part II: Topical Studies in Oceanography*, **49**, 403–462. The US JGOFS Synthesis  
526 and Modeling Project: Phase 1.
- 527 Moore, J. K., Doney, S. C. and Lindsay, K. (2004) Upper ocean ecosystem dynamics and iron cycling in a global three-  
528 dimensional model. *Global Biogeochemical Cycles*, **18**.
- 529 Ono, T., Midorikawa, T., Watanabe, Y. W., Tadokoro, K. and Saino, T. (2001) Temporal increases of phosphate and apparent  
530 oxygen utilization in the subsurface waters of western subarctic Pacific from 1968 to 1998. *Geophysical Research Letters*,  
531 **28**, 3285–3288.
- 532 Oschlies, A. (2021) A committed fourfold increase in ocean oxygen loss. *Nature Communications*, **12**, 2307.
- 533 Palacios-Abrantes, J., Reygondeau, G., Wabnitz, C. C. C. and Cheung, W. W. L. (2020) The transboundary nature of the world's  
534 exploited marine species. *Scientific Reports*, **10**, 17668.
- 535 Perry, A. L., Low, P. J., Ellis, J. R. and Reynolds, J. D. (2005) Climate change and distribution shifts in marine fishes. *Science*,  
536 **308**, 1912–1915.
- 537 Perry, R. I., Dilke, B. R. and Parsons, T. R. (1983) Tidal mixing and summer plankton distributions in Hecate Strait, British  
538 Columbia. *Canadian Journal of Fisheries and Aquatic Sciences*, **40**, 871–887.
- 539 Pörtner, H. O. and Knust, R. (2007) Climate change affects marine fishes through the oxygen limitation of thermal tolerance.  
540 *Science*, **315**, 95–97.
- 541 Renault, L., McWilliams, J. C., Kessouri, F., Jousse, A., Frenzel, H., Chen, R. and Deutsch, C. (2021) Evaluation of high-resolution  
542 atmospheric and oceanic simulations of the California Current System. *Progress in Oceanography*, **195**, 102564.
- 543 Rooper, C. N., Ortiz, I., Hermann, A. J., Laman, N., Cheng, W., Kearney, K. and Aydin, K. (2020) Predicted shifts of groundfish  
544 distribution in the Eastern Bering Sea under climate change, with implications for fish populations and fisheries manage-  
545 ment. *ICES Journal of Marine Science*, **78**, 220–234.
- 546 Ross, T., Du Preez, C. and Ianson, D. (2020) Rapid deep ocean deoxygenation and acidification threaten life on Northeast  
547 Pacific seamounts. *Global Change Biology*, **26**, 6424–6444.
- 548 Sadorus, L., Walker, J. and Sullivan, M. (2016) IPHC oceanographic data collection program 2000-2014. Int. Pac. Halibut  
549 Comm. Tech. Rep. 60.

- 550 Sadorus, L. L., Goldstein, E. D., Webster, R. A., Stockhausen, W. T., Planas, J. V. and Duffy-Anderson, J. T. (2021) Multiple  
551 life-stage connectivity of Pacific halibut (*Hippoglossus stenolepis*) across the Bering Sea and Gulf of Alaska. *Fisheries*  
552 *Oceanography*, **30**, 174–193.
- 553 Sadorus, L. L., Mantua, N. J., Essington, T., Hickey, B. and Hare, S. (2014) Distribution patterns of Pacific halibut (*Hippoglossus*  
554 *stenolepis*) in relation to environmental variables along the continental shelf waters of the US West Coast and southern  
555 British Columbia. *Fisheries Oceanography*, **23**, 225–241.
- 556 Sasano, D., Takatani, Y., Kosugi, N., Nakano, T., Midorikawa, T. and Ishii, M. (2018) Decline and bidecadal oscillations of  
557 dissolved oxygen in the Oyashio region and their propagation to the western North Pacific. *Global Biogeochemical Cycles*,  
558 **32**, 909–931.
- 559 Schmidtko, S., Stramma, L. and Visbeck, M. (2017) Decline in global oceanic oxygen content during the past five decades.  
560 *Nature*, **542**, 335–339.
- 561 Schwalm, C. R., Glendon, S. and Duffy, P. B. (2020) RCP8.5 tracks cumulative CO<sub>2</sub> emissions. *Proceedings of the National*  
562 *Academy of Sciences*, **117**, 19656–19657.
- 563 Seibel, B. A. (2011) Critical oxygen levels and metabolic suppression in oceanic oxygen minimum zones. *Journal of Experimental*  
564 *Biology*, **214**, 326–336.
- 565 Shawe-Taylor, J. and Cristianini, N. (2004) *Kernel Methods for Pattern Analysis*. Cambridge University Press.
- 566 Shchepetkin, A. F. and McWilliams, J. C. (2005) The regional oceanic modeling system (ROMS): a split-explicit, free-surface,  
567 topography-following-coordinate oceanic model. *Ocean Modelling*, **9**, 347–404.
- 568 Skud, B. (1977) Drift, migration, and intermingling of Pacific halibut stocks. *Int. Pac. Halibut Comm. Sci. Rep.*, **63**, 42.
- 569 Stewart, I., H. A. W. R. and Wilson, D. (2020) Summary of the data, stock assessment, and harvest decision table for Pacific  
570 halibut (*Hippoglossus stenolepis*) at the end of 2019. *Int. Pac. Halibut Comm. Annual Meeting Report*, IPHC-2020-AM096-  
571 09 Rev2.
- 572 Sumaila, U. R., Cheung, W. W. L., Lam, V. W. Y., Pauly, D. and Herrick, S. (2011) Climate change impacts on the biophysics and  
573 economics of world fisheries. *Nature Climate Change*, **1**, 449–456.
- 574 Sumaila, U. R., Tai, T. C., Lam, V. W. Y., Cheung, W. W. L., Bailey, M., Cisneros-Montemayor, A. M., Chen, O. L. and Gulati, S. S.  
575 (2019) Benefits of the Paris Agreement to ocean life, economies, and people. *Science Advances*, **5**, eaau3855.
- 576 Sumaila, U. R. and VanderZwaag, D. L. (2020) Canada and transboundary fisheries management in changing oceans: taking  
577 stock, future scenarios. *Ecology and Society*, **25**, 44.
- 578 Sunday, J. M., Pecl, G. T., Frusher, S., Hobday, A. J., Hill, N., Holbrook, N. J., Edgar, G. J., Stuart-Smith, R., Barrett, N., Wernberg,  
579 T., Watson, R. A., Smale, D. A., Fulton, E. A., Slawinski, D., Feng, M., Radford, B. T., Thompson, P. A. and Bates, A. E.  
580 (2015) Species traits and climate velocity explain geographic range shifts in an ocean-warming hotspot. *Ecology Letters*,  
581 **18**, 944–953.
- 582 Thompson, P. L., Nephin, J., Davies, S. C., Park, A. E., Lyons, D. A., Rooper, C. N., Peña, M. A., Christian, J. R., Hunter, K. L.,  
583 Rubidge, E. and Holdsworth, A. M. (2022) Groundfish biodiversity change in northeastern Pacific waters under projected  
584 warming and deoxygenation. *bioRxiv*.
- 585 Thompson, W. L., White, G. C. and Gowan, C. (1998) Chapter 7 - Fish. In *Monitoring Vertebrate Populations* (eds. W. L. Thomp-  
586 son, G. C. White and C. Gowan), 191–232. San Diego: Academic Press.
- 587 Ware, D. and McFarlane, G. (1989) Fisheries production domains in the northeast Pacific Ocean. In *Effects of ocean variability*  
588 *on recruitment and an evaluation of parameters used in stock assessment models* (eds. R. Beamish and G. McFarlane), 359–379.  
589 *Can. Spec. Publ. Fish. Aquat. Sci.*

- 590 Yati, E., Minobe, S., Mantua, N., Ito, S.-i. and Di Lorenzo, E. (2020) Marine ecosystem variations over the North Pacific and  
591 their linkage to large-scale climate variability and change. *Frontiers in Marine Science*, **7**, 925.
- 592 Youcef, W. A., Lambert, Y. and Audet, C. (2015) Variations in length and growth of Greenland Halibut juveniles in relation to  
593 environmental conditions. *Fisheries Research*, **167**, 38–47.